PAPER

NJC
www.rsc.org/njc

Synthesis and structures of new oligomethylene-bridged double ladders. How far can the layers be separated?†‡

Jens Beckmann,[a] Dainis Dakternieks,*[a] Andrew Duthie,[a] Fong Sheen Kuan,[a] Klaus Jurkschat,*[b] Markus Schürmann[b] and Edward R. T. Tiekink*[c]

[a] *Centre for Chiral and Molecular Technologies, Deakin University, Geelong, 3217 Australia*
[b] *Lehrstuhl für Anorganische Chemie II, Universität Dortmund, 44221 Dortmund, Germany*
[c] *Department of Chemistry, National University of Singapore, Singapore 11754*

Received (in Montpellier, France) 8th December 2003, Accepted 5th May 2004
First published as an Advance Article on the web 16th September 2004

The synthesis of the α,ω-bis[dichloro(trimethylsilylmethyl)stannyl]alkanes, $(Me_3SiCH_2)Cl_2Sn(CH_2)_nSnCl_2(CH_2SiMe_3)$ (**13**, $n = 5$; **14**, $n = 6$; **15**, $n = 7$; **16**, $n = 8$; **17**, $n = 10$; **18**, $n = 12$) and the corresponding oligomethylene-bridged diorganotin oxides $[(Me_3SiCH_2)(O)Sn(CH_2)_nSn(O)(CH_2SiMe_3)]_m$ (**19**, $n = 5$; **20**, $n = 6$; **21**, $n = 7$; **22**, $n = 8$; **23**, $n = 10$; **24**; $n = 12$) is reported. The reaction of the diorganodichlorostannanes **13**–**18** with the corresponding diorganotin oxides **19**–**24** provided the spacer-bridged tetraorganodistannoxanes $\{[(Me_3SiCH_2)ClSn(CH_2)_nSnCl(CH_2SiMe_3)]O\}_4$ (**25**, $n = 5$; **26**, $n = 6$; **27**, $n = 7$; **28**, $n = 8$; **29**, $n = 10$; **30**, $n = 12$). Compounds **13**–**30** have been identified by elemental analyses and multinuclear NMR spectroscopy. Compounds **25**, **27**, **29** and **30** have also been characterised by single crystal X-ray diffraction analysis and electrospray mass spectrometry. For the latter the essential double ladder motif is maintained for all *n* in the solid state, but subtle changes in alignment of the ladder planes occur. Separation between the two layers of the double ladder ranges from approx. 8.7 Å (for **25**, $n = 5$) to approx. 15 Å (for **30**, $n = 12$). In solution there is some dissociation of the double ladders into the corresponding dimers. The degree of dissociation is favoured by increasing oligomethylene chain length *n*.

Introduction

Dimeric tetraorganodistannoxanes $[R_2(X)SnOSn(Y)R_2]_2$ (X, Y = Hal, OH, OCOR, OSO_2R, $OSiMe_3$; R = alkyl, aryl)[1] that possess a common ladder-like $Sn_4O_2X_2Y_2$ structural motif in the solid state (**A**, Chart 1) are currently under investigation as mild homogeneous catalysts for a variety of organic reactions, including transesterifications, selective acylation of alcohols, urethane formation and the ring-opening polymerisation of lactones.[2] The catalytic activity of these ladder compounds has been attributed to the kinetic lability and partial dissociation of the dimeric structure in solution to give monomers with a greater Lewis acidity.[3]

In previous work, we demonstrated that double ladder arrangements can be obtained by use of organic spacers and that these double ladders can be considered as new types of inorganic-organic hybrid oligomers featuring parallel $Sn_4O_2X_2Y_2$ units (**B**, Chart 1). The basic layer structure of double ladders is tolerant to a great variety of different organic spacers, for example, $-(CH_2)_n-$ ($n = 1$–4), –(*p*- or *m*-$CH_2SiMe_2C_6H_4CH_2SiMe_2$)– and –[*p*- or *m*-$(CH_2)_2C_6H_4(CH_2)_2$]–.[4] The choice of the organic spacers allows modifications of the geometric features such as (*i*) layer separation, (*ii*) cavity size, (*iii*) twist of the layers, (*iv*) chirality and may also allow incorporation of functional groups, such as ether moieties,[5] into the framework. In continuation of this work we now describe the use of very long oligomethylene spacer-linked ditin precursors with up to twelve carbon atoms. Inorganic-organic hybrid clusters with tailor-made shapes and sizes may find applications as intercalates for pillared clay minerals, such as montmorillonite, to give nanocomposite materials with modified qualities.[6]

Results and discussion

Synthetic aspects

The synthesis of ditin precursors was achieved following the reaction sequence outlined in Scheme 1. Starting from α,ω-bis(triphenylstannyl)alkane, $Ph_3Sn(CH_2)_nSnPh_3$, one phenyl group at each tin atom was selectively cleaved using iodine to provide the respective α,ω-bis(iododiphenylstannyl)alkanes, $IPh_2Sn(CH_2)_nSnPh_2I$ (**1**–**6**; $n = 5$–8, 10, 12). To assist with crystallisation of the double ladders, the trimethylsilylmethyl group was introduced by reaction of **1**–**6** with 2 equiv of Me_3SiCH_2MgCl, affording the corresponding α,ω-bis[(trimethylsilylmethyl)diphenylstannyl]alkanes, $(Me_3SiCH_2)Ph_2Sn(CH_2)_nSnPh_2(CH_2SiMe_3)$ (**7**–**12**; $n = 5$–8, 10, 12). All remaining phenyl groups were then cleaved, using an excess of concentrated hydrochloric acid, to give the respective α,ω-bis[(trimethylsilylmethyl)dichlorostannyl]alkanes, $(Me_3SiCH_2)Cl_2Sn(CH_2)_nSnCl_2(CH_2SiMe_3)$ (**13**–**18**; $n = 5$–8, 10, 12). A portion of the latter was hydrolysed to produce the corresponding spacer-bridged diorganotin oxides $[(Me_3SiCH_2)(O)Sn(CH_2)_nSn(O)(CH_2SiMe_3)]_m$ (**19**–**24**; $n = 5$–8, 10, 12).

Compounds **1**–**18** are liquid or low-melting materials that are very soluble in most organic solvents, whereas compounds **19**–**24** are insoluble, high-melting solids, presumably due to their polymeric nature.[7] Compounds **1**–**24** were characterised in most cases by elemental analysis and ^{119}Sn NMR spectroscopy; these data are collected along with preparative yields in Table 1. Additional ^1H and ^{13}C NMR data are given in the Electronic supplementary information (ESI).

The double ladders $\{[(Me_3SiCH_2)ClSn(CH_2)_nSnCl(CH_2SiMe_3)]O\}_4$ (**25**–**30**; $n = 5$–8, 10, 12) were prepared by the reaction of equimolar amounts of the α,ω-bis

† Dedicated to the occasion of the 70th birthday of Professor Reinhard Schmutzler.
‡ Electronic supplementary information (ESI) available: ^1H and ^{13}C NMR data (in $CDCl_3$) of compounds **1**–**18** and **25**–**30**. See http://www.rsc.org/suppdata/nj/b3/b316009b/

DOI: 10.1039/b316009b

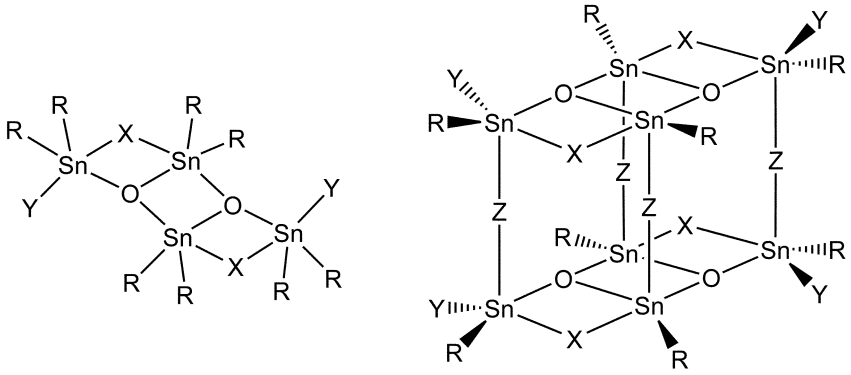

(**A**) (**B**)

X, Y = Hal, OH, OCOR, OSO_2R, $OSiMe_3$; R = alkyl, aryl

Chart 1

[(trimethylsilylmethyl)dichlorostannyl]alkanes **13**–**18** with the corresponding spacer-bridged diorganotin oxides **19**–**24** of the same space length [eqn. (1)]:

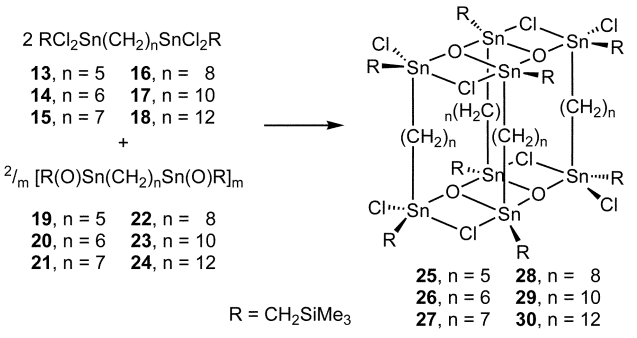

2 $RCl_2Sn(CH_2)_nSnCl_2R$

13, n = 5 **16**, n = 8
14, n = 6 **17**, n = 10
15, n = 7 **18**, n = 12

+

$^2/_m$ $[R(O)Sn(CH_2)_nSn(O)R]_m$

19, n = 5 **22**, n = 8
20, n = 6 **23**, n = 10
21, n = 7 **24**, n = 12

$R = CH_2SiMe_3$

25, n = 5 **28**, n = 8
26, n = 6 **29**, n = 10
27, n = 7 **30**, n = 12

(1)

Molecular structures of 25, 27, 29 and 30

The molecular structure of **25** is shown in Fig. 1 and key geometric parameters for this and for structures **27**, **29** and **30** are collected in Table 2. The structure conforms to the expected motif in that two tetraorganodistannoxane units are linked *via* a common Sn_2O_2 core with additional bridges between the endo- and exocyclic tin atoms being provided by two chlorides, with the two remaining chlorides occupying terminal positions at the two exocyclic tin atoms. Two such essentially planar (mean deviation 0.14 Å) $Sn_4O_2Cl_4$ entities are linked *via* $–(CH_2)_5–$ spacers so that pairs of endocyclic tin atoms are connected by common chains, as are the exocyclic tin atoms. The $–CH_2SiMe_3$ groups in effect cap the $\{Sn_4O_2Cl_4[(CH_2)_5]_4Sn_4O_2Cl_4\}$ molecular box thus formed. The overall molecular symmetry is centrosymmetric, with the centre being at the centre of gravity of the molecule, so that the two $Sn_4O_2Cl_4$ faces are parallel and directly superimposable. The average separation between the $Sn_4O_2Cl_4$ faces is 8.7 Å. The chloride bridges are to a first approximation symmetric and the Sn–Cl terminal bond distances are shorter than the bridging Sn–Cl distances (Table 2). The coordination geometry for the

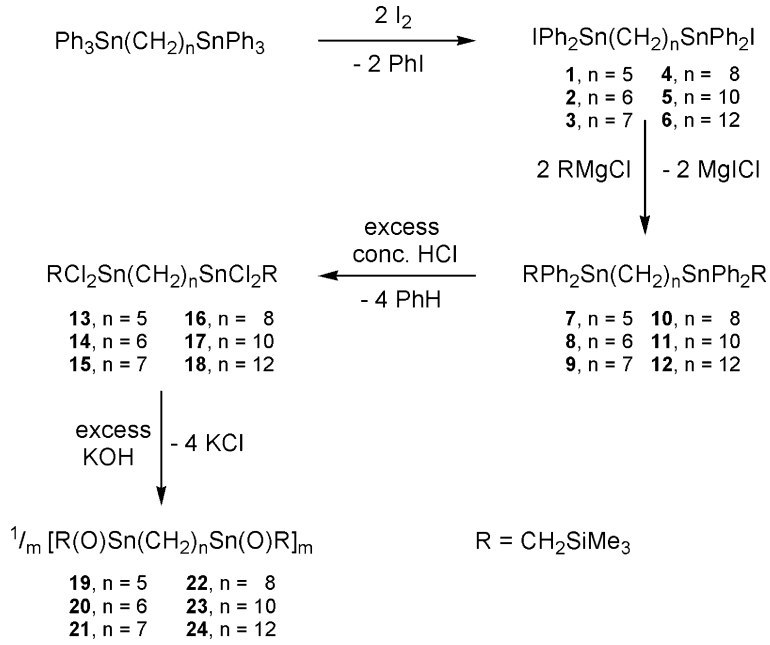

$Ph_3Sn(CH_2)_nSnPh_3$ —(2 I_2, - 2 PhI)→ $IPh_2Sn(CH_2)_nSnPh_2I$

1, n = 5 **4**, n = 8
2, n = 6 **5**, n = 10
3, n = 7 **6**, n = 12

2 RMgCl | - 2 MgICl

$RPh_2Sn(CH_2)_nSnPh_2R$ —(excess conc. HCl, - 4 PhH)→ $RCl_2Sn(CH_2)_nSnCl_2R$

7, n = 5 **10**, n = 8
8, n = 6 **11**, n = 10
9, n = 7 **12**, n = 12

13, n = 5 **16**, n = 8
14, n = 6 **17**, n = 10
15, n = 7 **18**, n = 12

excess KOH | - 4 KCl

$^1/_m$ $[R(O)Sn(CH_2)_nSn(O)R]_m$ $R = CH_2SiMe_3$

19, n = 5 **22**, n = 8
20, n = 6 **23**, n = 10
21, n = 7 **24**, n = 12

Scheme 1

Table 1 Analytical and physical data for **1**–**30** (R = CH_2SiMe_3)

Compound	Yield (%)	Mp/°C	^{119}Sn NMR/ppm[d]	C, H Analysis (%)	
				C (calcd)	H (calcd)
$IPh_2Sn(CH_2)_5SnPh_2I$ (**1**)	>95[a]	–[c]	−51.5		
$IPh_2Sn(CH_2)_6SnPh_2I$ (**2**)	>95[a]	–[c]	−50.7		
$IPh_2Sn(CH_2)_7SnPh_2I$ (**3**)	>95[a]	–[c]	−50.7		
$IPh_2Sn(CH_2)_8SnPh_2I$ (**4**)	>95[a]	–[c]	−52.0		
$IPh_2Sn(CH_2)_{10}SnPh_2I$ (**5**)	>95[a]	–[c]	−51.9		
$IPh_2Sn(CH_2)_{12}SnPh_2I$ (**6**)	>95[a]	–[c]	−51.8		
$RPh_2Sn(CH_2)_5SnPh_2R$ (**7**)	>95[a]	–[c]	−58.4		
$RPh_2Sn(CH_2)_6SnPh_2R$ (**8**)	>95[a]	–[c]	−58.7		
$RPh_2Sn(CH_2)_7SnPh_2R$ (**9**)	>95[a]	–[c]	−58.6		
$RPh_2Sn(CH_2)_8SnPh_2R$ (**10**)	>95[a]	–[c]	−58.8		
$RPh_2Sn(CH_2)_{10}SnPh_2R$ (**11**)	>95[a]	–[c]	−58.6		
$RPh_2Sn(CH_2)_{12}SnPh_2R$ (**12**)	>95[a]	–[c]	−58.4		
$RCl_2Sn(CH_2)_5SnCl_2R$ (**13**)	68[b]	41–43	138.8	24.95 (25.03)	5.25 (5.17)
$RCl_2Sn(CH_2)_6SnCl_2R$ (**14**)	75[b]	49–52	138.9	26.32 (26.36)	5.24 (5.37)
$RCl_2Sn(CH_2)_7SnCl_2R$ (**15**)	71[b]	43–45	138.2	27.46 (27.64)	5.50 (5.57)
$RCl_2Sn(CH_2)_8SnCl_2R$ (**16**)	65[b]	27–28	138.3	28.80 (28.86)	5.85 (5.75)
$RCl_2Sn(CH_2)_{10}SnCl_2R$ (**17**)	73[b]	45–46	138.9	31.35 (31.15)	6.05 (6.10)
$RCl_2Sn(CH_2)_{12}SnCl_2R$ (**18**)	67[b]	36–37	138.1	33.27 (33.50)	6.42 (6.50)
$[R(O)Sn(CH_2)_5Sn(O)R]_m$ (**19**)	94	>350	Insoluble	30.17 (30.38)	6.18 (6.28)
$[R(O)Sn(CH_2)_6Sn(O)R]_m$ (**20**)	93	>270	Insoluble	31.85 (31.95)	6.49 (6.15)
$[R(O)Sn(CH_2)_7Sn(O)R]_m$ (**21**)	99	>300	Insoluble	33.33 (33.24)	6.55 (6.69)
$[R(O)Sn(CH_2)_8Sn(O)R]_m$ (**22**)	96	>350	Insoluble	34.25 (34.56)	6.60 (6.89)
$[R(O)Sn(CH_2)_{10}Sn(O)R]_m$ (**23**)	92	>350	Insoluble	36.65 (37.01)	7.00 (7.25)
$[R(O)Sn(CH_2)_{12}Sn(O)R]_m$ (**24**)	95	>350	Insoluble	38.90 (39.24)	7.20 (7.57)
$\{[RClSn(CH_2)_5SnClR]O\}_4$ (**25**)	96	294-295	−86.9/−130.9 (DL: 100%)	29.68 (29.93)	6.11 (5.79)
$\{[RClSn(CH_2)_6SnClR]O\}_4$ (**26**)	85	245–247	−71.8/−137.2 (DL: 90%); −81.0/−137.0 (L: 10%)	28.67 (28.85)	5.82 (5.88)
$\{[RClSn(CH_2)_7SnClR]O\}_4$ (**27**)	80	296–297	−84.3/−132.6 (DL: 85%); −81.0/−136.5 (L: 15%)	30.28 (30.18)	6.07 (6.08)
$\{[RClSn(CH_2)_8SnClR]O\}_4$ (**28**)	52	245–246	−75.6/−136.6 (DL: 75%); −75.9/−137.4 (L: 25%)	31.40 (31.45)	6.25 (6.27)
$\{[RClSn(CH_2)_{10}SnClR]O\}_4$ (**29**)	43	229–231	−78.6/−136.3 (DL: 67%); −78.9/−137.2 (L: 33%)	33.88 (33.83)	6.52 (6.62)
$\{[RClSn(CH_2)_{12}SnClR]O\}_4$ (**30**)	35	216–218	−80.5/−136.2 (DL: 60%); −80.6/−136.9 (L: 40%)	36.10 (36.01)	6.90 (6.95)

[a] For compounds **1**–**6** and **7**–**12** yields are as measured by ^{119}Sn NMR spectroscopy. [b] Yields (isolated) for compounds **13**–**18** are for three synthetic steps. [c] Compound is an oil at room temperature. No mp was determined. [d] L = ladder and DL = double ladder.

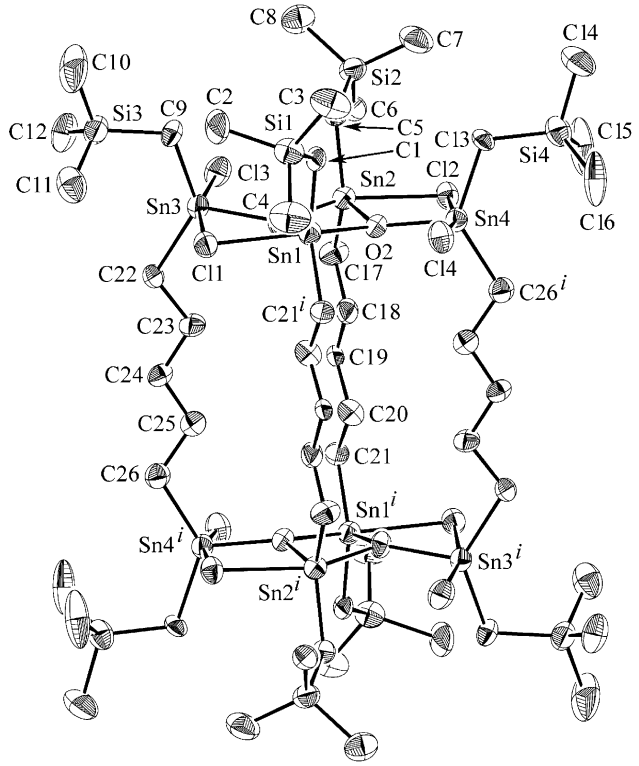

Fig. 1 Molecular structure of centrosymmetric **25** showing the atomic numbering scheme. Hydrogen atoms have been removed for reasons of clarity. Symmetry transformation used to generate equivalent atoms: $i = 1-x, 1-y, -z$.

five-coordinate exocyclic tin atoms is trigonal bipyramidal with the axial positions being occupied by the chlorides from the C_2OCl_2 donor set. The geometry of the endocyclic tin atoms is also distorted trigonal bipyramidal but with a chloride and an oxygen atom occupying axial positions. The intermolecular $Sn_1\cdots Cl_3$ and $Sn_2\cdots Cl_4$ distances are greater than 3.4 Å and as such are not considered to form bonding interactions.

The crystal structure of **25** comprises regular stacking of the molecular parallelepipeds so that simply, molecules stack on top of each other separated by hydrophobic interactions involving, in the main, the CH_2SiMe_2 groups. Adjacent columns are similarly connected *via* hydrophobic interactions so that the lattice can be described as simple orthogonal packing of boxes in three dimensions. Fig. 2(a) shows a representation of the crystal lattice found for **25**.

The molecular structure of **27**, the $-(CH_2)_7-$ analogue, is shown in Fig. 3 and exhibits the same structural features as for **25**, being centrosymmetric, but is not isomorphous. The mean deviation of the atoms defining the $Sn_4O_2Cl_4$ face is 0.12 Å and the average separation between these parallel faces is 12.3 Å. The crystal packing in **27** is quite distinct from that described for **25**. In the lattice of **27**, the molecules within the columns defined for **25**, Fig. 2(a), are off-set laterally by half a molecule and, similarly, the molecules in the columns are off-set by half a molecule with respect to neighbouring columns, as represented in Fig. 2(b).

Increasing the length of the spacer to ten methylene groups, as in **29**, sees retention of the basic molecular motif described above, see Fig. 4, but with some differences that are probably related to the increased flexibility in the spacer. The molecule has crystallographic two-fold symmetry, with the axis passing through the oligomethylene spacers. The two faces, each planar

Table 2 Geometric parameters (°, Å) for **25**, **27**, **29** and **30**

	25	**27**	**29** · 5(toluene)	**30** · 2(toluene)
Sn_1–O_1	2.039(10)	2.046(4)	2.037(6)	2.056(2)
Sn_1–O_2	2.150(10)	2.151(4)	2.138(6)	2.120(3)
Sn_1–Cl_1	2.641(5)	2.658(2)	2.660(3)	2.826(2)
Sn_2–O_1	2.122(10)	2.165(4)	2.151(6)	2.106(3)
Sn_2–O_2	2.028(10)	2.047(4)	2.042(6)	2.040(3)
Sn_2–Cl_2	2.629(4)	2.627(2)	2.662(3)	3.090(1)
Sn_3–O_1	2.048(10)	2.009(5)	2.023(6)	2.024(2)
Sn_3–Cl_1	2.744(5)	2.788(4)	2.800(3)	2.650(1)
Sn_3–Cl_3	2.455(5)	2.438(5)	2.454(3)	2.518(1)
Sn_4–O_2	2.045(10)	2.010(4)	2.025(6)	2.016(2)
Sn_4–Cl_2	2.780(4)	2.820(2)	2.744(3)	2.607(2)
Sn_4–Cl_4	2.448(5)	2.443(2)	2.468(3)	2.547(2)
O_1–Sn_1–O_2	72.6(4)	74.3(1)	73.9(2)	73.8(1)
O_1–Sn_1–Cl_1	77.9(3)	78.3(1)	79.1(2)	73.64(8)
O_2–Sn_1–Cl_1	149.9(3)	152.4(1)	152.7(2)	147.46(7)
O_1–Sn_2–O_2	73.4(4)	73.9(1)	73.5(2)	74.4(1)
O_1–Sn_2–Cl_2	151.7(3)	153.2(1)	151.2(2)	71.94(9)
O_2–Sn_2–Cl_2	78.9(3)	79.5(1)	77.8(2)	146.38(7)
O_1–Sn_3–Cl_1	75.3(3)	75.7(2)	75.9(2)	78.28(8)
O_1–Sn_3–Cl_3	89.6(3)	90.9(2)	90.1(2)	83.42(8)
Cl_1–Sn_3–Cl_3	164.6(2)	166.4(2)	165.15(10)	161.20(4)
O_2–Sn_4–Cl_2	75.0(3)	75.4(1)	76.1(2)	80.34(9)
O_2–Sn_4–Cl_4	91.5(3)	89.5 (1)	88.7(2)	84.86(9)
Cl_2–Sn_4–Cl_4	165.9(2)	164.6 (1)	164.29(10)	164.17(4)

to 0.06 Å, are still effectively parallel but twisted approximately 41° with respect to each other. The average distance between faces is 14.8 Å. In all other respects, such as in the nature of the

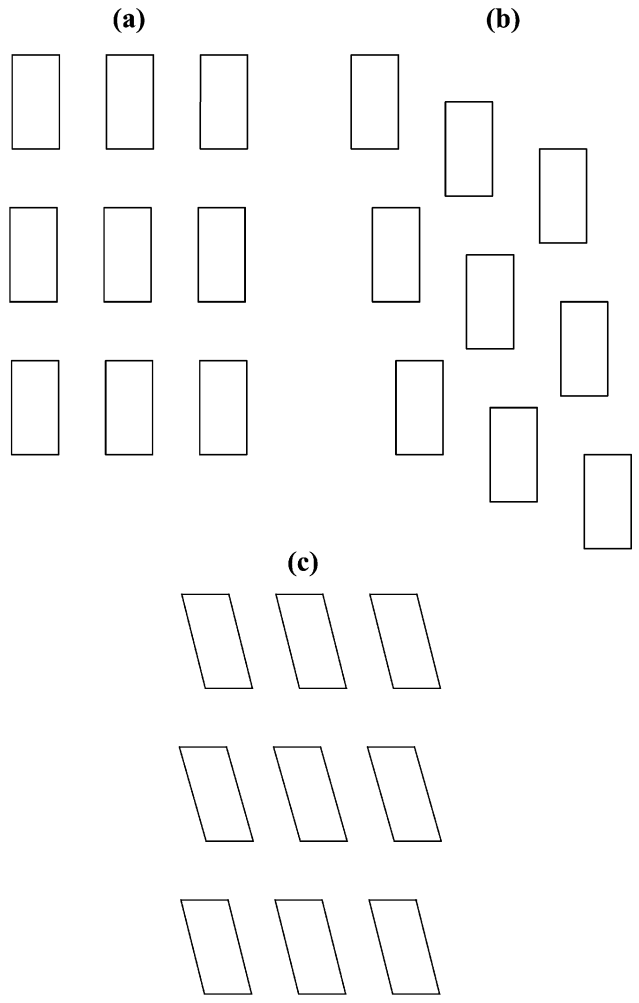

Fig. 2 Schematic diagrams representing the molecular packing in (a) **25** and **29** · 5(toluene), (b) **27**, and (c) **30** · 2(toluene).

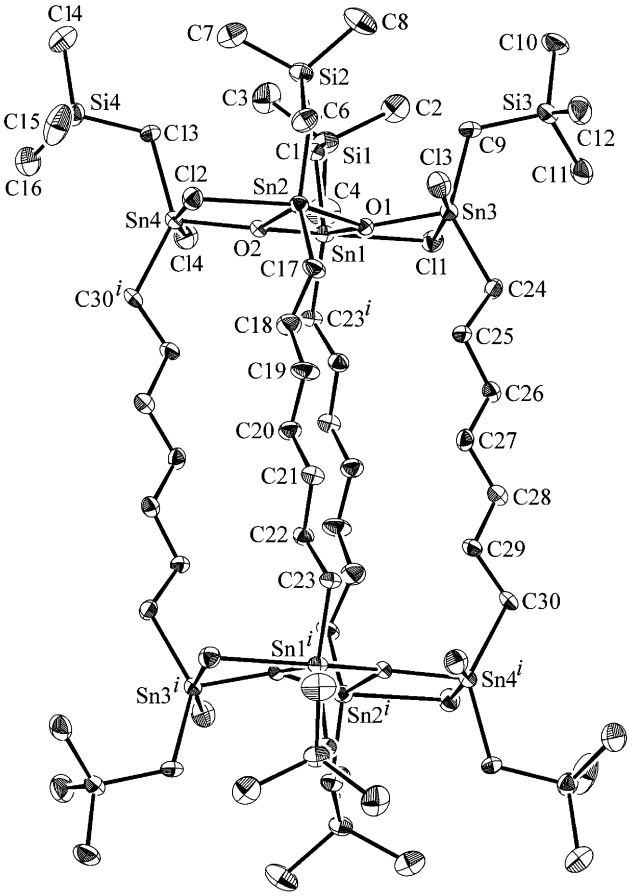

Fig. 3 Molecular structure of centrosymmetric **27** showing the atomic numbering scheme. Hydrogen atoms have been removed for reasons of clarity. Symmetry transformation used to generate equivalent atoms: $i = -x, -y, -z$.

molecular connectivity, the structure of **29** resembles those described above (Table 2). The crystal lattice of **29** contains solvent toluene molecules so that for each molecule of **29**, there are five toluene molecules. The solvent is not incorporated within the molecular framework but rather exists in regions surrounding the spacer ligands of adjacent molecules. In fact, the crystal packing in **29** resembles almost exactly that described for **25**, Fig. 2(a), but with solvent molecules occupying regions between the columns so that the global crystal packing is not affected to any great extent by the inclusion of solvent.

By contrast to the preceding three structures, some significant structural changes are evident for **30**. As apparent from Fig. 5, the description of the molecular structures of **25**, **27** and **29** as molecular rectangular boxes is no longer strictly applicable for **30** as there is definite skewing in the molecular polygon. Molecules of **30** are centrosymmetric so that the $Sn_4O_2Cl_4$ planes are parallel but there is some significant buckling in the links at the Sn_1 and Sn_4 atoms so that there is no superimposition of the two faces. The relationships between the four structures in terms of the relative orientations of the $Sn_4Cl_4O_2$ faces are conveniently summarised in Fig. 6 where the top $Sn_4Cl_4O_2$ face is projected normal to the plane through these atoms. For structure **25** (and **27**), it is evident that the faces are superimposable. By contrast, in molecule **29**, the faces are of opposite orientation but lie on top of each other. Finally, in **30**, the faces, while of the same orientation as found in **25** and **27**, are somewhat displaced with respect to each other. The displacement can be rationalised by considering the conformation of the linking alkyl groups. The individual links within the alkyl spacers all have the open or trans conformation; the maximum deviation of any of the C–C–C–C torsion angles from 180° is 171.9(4)°. This pattern extends to

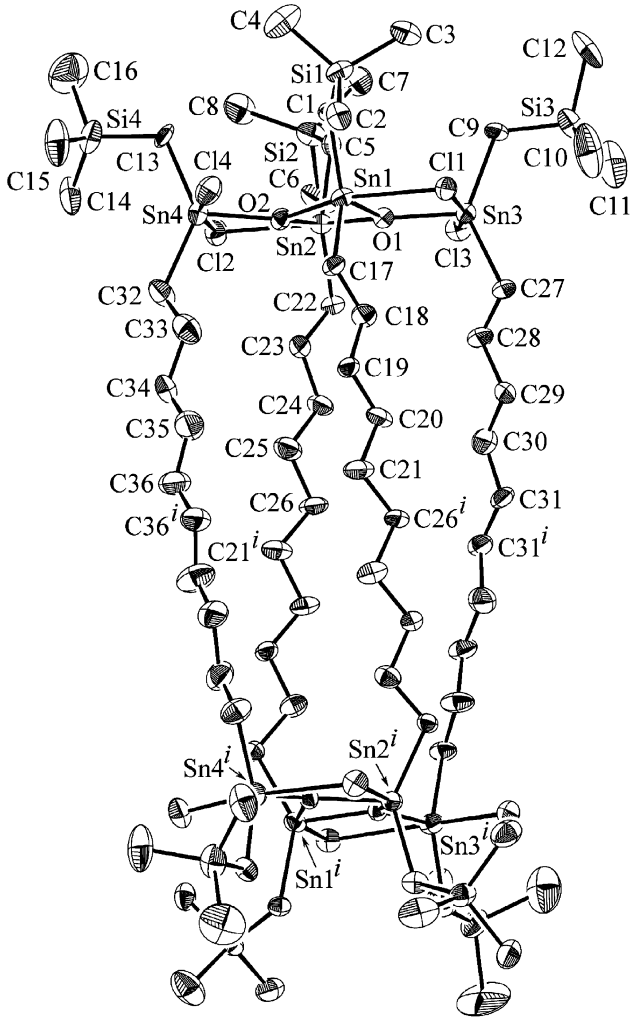

Fig. 4 Molecular structure of **29** in **29** · 5(toluene), showing the atomic numbering scheme. The molecule has crystallographically imposed two-fold symmetry. Hydrogen atoms have been removed for reasons of clarity. Symmetry transformation used to generate equivalent atoms: $i = -x, y, -\frac{1}{2} - z$.

include the Sn_2 and Sn_3 atoms, as seen in the respective Sn–C–C–C torsion angles of −167.8(3)° and 175.6(3)°, but not to the Sn_1 and Sn_4 atoms, as reflected in the respective Sn–C–C–C torsion angles of −67.3(4)° and 74.7(6)°. This has the effect of tilting the faces as shown in Fig. 5. The question then arises: is there a chemical reason behind this arrangement?

The major difference in the molecular dimensions defining the $Sn_4O_2Cl_4$ plane pertains to the nature of the Sn–Cl contacts. In each of **25**, **27** and **29** there are two almost symmetric Sn–Cl–Sn bridges and no significant interactions between the endocyclic tin atoms and the terminal chlorides. By contrast, in **30**, a different situation pertains as the $Sn_{endocylic}$–Cl distances are Sn_1–Cl_1 2.826(2) Å, Sn_1–Cl_4 3.139(2) Å, Sn_2–Cl_2 3.090(1) Å and Sn_2–Cl_3 2.942(2) Å; these are not shown in Fig. 5. Taken to an extreme, that is if these contacts are not considered significant, the endocyclic tin atoms may be considered as being four-coordinate, distorted tetrahedral as opposed to octahedral if they were considered significant. A similar situation is observed for the simple ladder compound $[Me_2(Cl)SnOSn(Cl)Me_2]_2$ in the co-crystallisate with $[PtClMe_2(SnCl_3)(bu_2bpy)]$ (Bu_2bpy = 4,4′-di-*tert*-butyl-2,2′-bipyridine), where it shows four crystallographically related $Sn_{endocylic}$–Cl distances of 3.015(2) Å.[8] However, by itself the structure of $[Me_2(Cl)SnOSn(Cl)Me_2]_2$ reveals two crystallographically related $Sn_{endocylic}$–Cl distances of 2.702(2) and 3.409(2) Å.[9] The pattern observed for **30** is distinctly different from that found in the structures of the lower congeners; the exocyclic tin atoms

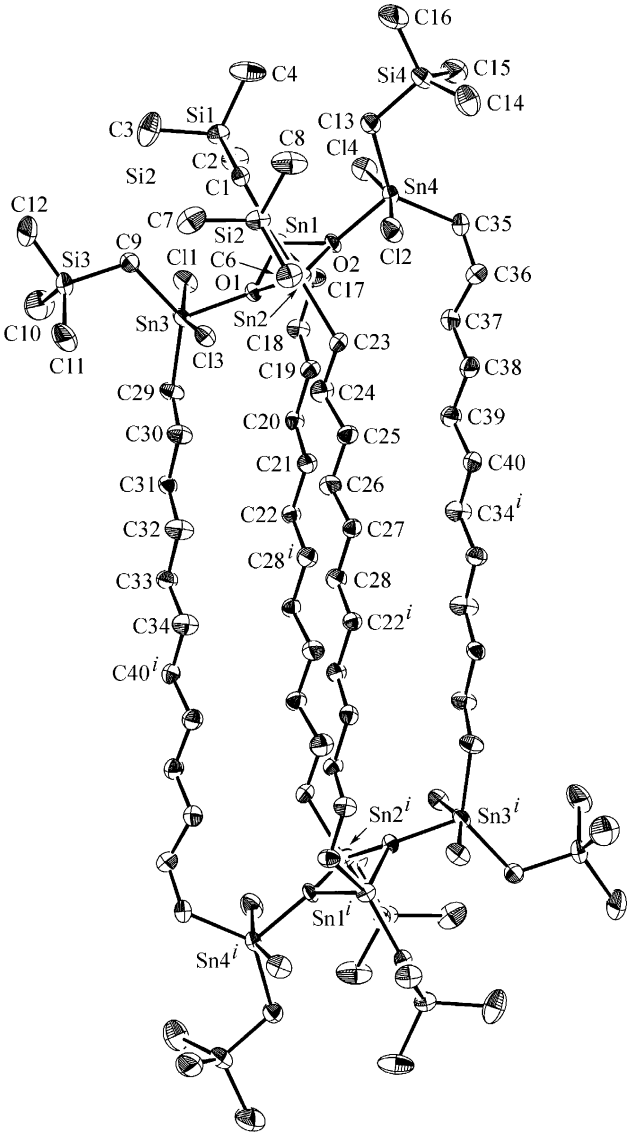

Fig. 5 Molecular structure of centrosymmetric **30** in **30** · 2(toluene), showing the atomic numbering scheme; the C5 atom is obscured. Hydrogen atoms have been removed for reasons of clarity. Symmetry transformation used to generate equivalent atoms: $i = -x, 1 - y, 2 - z$.

remain five-coordinate in all four structures. However, the tilting in the structure involves centrosymmetrically related pairs of endo- (Sn_1) and exocyclic (Sn_4) tin atoms so the difference in molecular connectivity revolving around the chlorides is unlikely to be the source of the disparity between the overall shapes of the molecular polygons. Compound **30** crystallises with two solvent molecules of toluene per molecule of **30**, but there are no noteworthy interactions between these components of the crystal. The crystal packing of **30** is based upon that described for **29**, which was, in turn, related back to **25**. The only difference is the tilting evident in the molecules as represented schematically in Fig. 2(c). Given that there is great scope for molecular flexibility in these molecules and that there are no inherent reasons for the adoption of molecular rectangles, it is possible that the energetics of crystal lattice formation may play a role in determining the molecular structure, but there is no experimental evidence to support this conjecture.

Solution studies of 25–30

The oligomethylene-bridged double ladder clusters $\{[(Me_3SiCH_2)ClSn(CH_2)_nSnCl(CH_2SiMe_3)]O\}_4$ (**25**–**30**; n = 5–8, 10, 12) are moderately soluble in slightly polar organic solvents such as chloroform or toluene. For freshly prepared samples of **25**–**30** in $CDCl_3$, ^{119}Sn NMR spectroscopy reveals at first only two

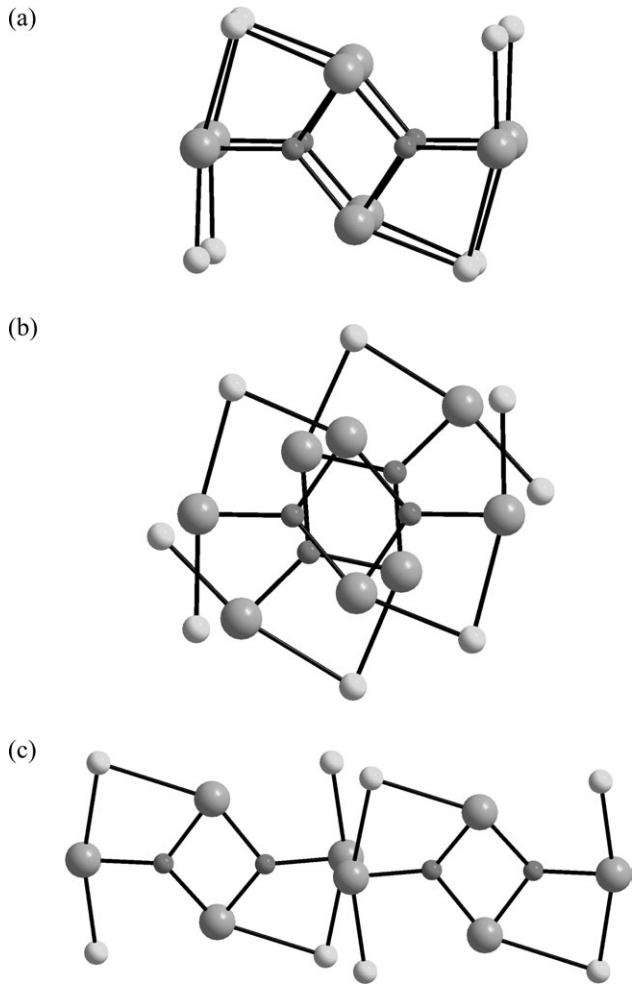

Fig. 6 View normal to the Sn_2O_2 plane of the superimposition of the top to bottom $Sn_4Cl_4O_2$ faces for: (a) **25** (the view for **27** is essentially identical), (b) **29**, and (c) **30**.

equally intense signals centred at $\delta - 79$ (deviation ± 8 ppm) and -134 (deviation ± 4 ppm), which are assigned to the exocyclic and endocyclic tin sites of the clusters, respectively.[10] Each of these signals shows identical $^2J(^{119}Sn–O–^{117}Sn)$ couplings of 65 Hz (deviation ± 1 Hz), consistent with the observed connectivity of the tin atoms.[10] The inequivalence of the exocyclic and endocyclic tin sites is further reflected by two different sets of ^1H and ^{13}C resonances (see ESI). After a few hours, ^{119}Sn NMR spectroscopy begins to show additional signals at -79 (deviation ± 3 ppm) and -137 (deviation ± 1 ppm) for $n \geq 6$, which are assigned to the ladder (L) compounds $\{[(Me_3SiCH_2)ClSn(CH_2)_nSnCl(CH_2SiMe_3)]O\}_2$ (**31**–**35**; $n = 6$–8, 10, 12), which are in equilibrium with the double ladder (DL) clusters **26**–**30** [eqn. (2)]:

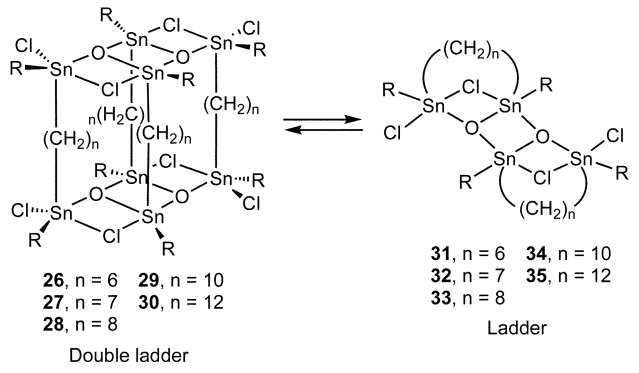

(2)

It is worth mentioning that a fluorine- as well as a benzoate-substituted analogue of this class of compound, namely $\{[(Me_3SiCH_2)_2CH(F)Sn(CH_2)_3Sn(F)CH(CH_2SiMe_3)_2]O\}_2$[11] and $\{[Me_3SiCH_2(PhCOO)Sn(CH_2)_3Sn(OCOPh)CH_2SiMe_3]O\}_2$ [4f], were described recently. After about 10 days the integral ratio of the ^{119}Sn NMR signals remains unchanged, which apparently suggests that a steady state concentration of the reactants (equilibrium) is reached at that time (Table 1). While the equilibrium for **26** and **31** ($n = 6$) stabilizes at 90 : 10, the proportion of ladder increases as the spacer length increases, so that for $n = 12$ the ratio between **30** and **35** is 60 : 40. Presumably this is due to longer spacers having a higher degree of flexibility. In order to confirm that water was not involved in the above equilibrium, a sample of **29** in dry toluene was prepared under inert conditions and flame-sealed. The ^{119}Sn NMR spectrum of this sample (5 min after dissolving) showed a DL-to-L ratio of 95 : 5. The ^{119}Sn NMR spectrum was again recorded after the sample had been maintained at 70 °C for 2 h. After heating the DL-to-L ratio changed to 70 : 30 (similar to that obtained for the sample kept at room temperature for 10 days). The IR spectrum (KBr) of the solid obtained after the removal of toluene contained no bands that could be associated with hydroxy groups.

It is also interesting to note that the preparative yield of the double ladders consistently decreases with increasing spacer length and goes from 96% to 35% on going from **25** ($n = 5$) to **30** ($n = 12$) (Table 1). In turn, there is evidence to suggest that the amount of higher oligomers and polymers in the crude reaction mixtures increases with increasing spacer chain length. The ^{119}Sn NMR spectra of crude reaction mixtures of **25**–**27** ($n = 5$–7) exhibit only sharp signals belonging to the corresponding ladder and double ladder; the reaction mixtures of **28**–**30** ($n = 8$, 10, 12) reveal broad signals in the regions -75 to -90 and -130 to -145, which are tentatively assigned to oligomeric and polymeric species. Integration shows that the amount of these species increases from about 40% for $n = 8$ to 60% for $n = 12$, suggesting that random cross-linking becomes more favoured with longer spacer lengths. It was necessary to perform the reactions for $n = 8$, 10, and 12 at high dilution (2–3 g L^{-1}) in order to obtain a higher proportion of ladder/double ladder to oligomer/polymer. The crude reaction mixtures from which the products **29** and **30** ($n = 10$, 12) had been removed were investigated to determine if there is an equilibrium at higher temperatures that would result in further product formation. However, after prolonged heating in refluxing toluene no changes in composition were observed (by ^{119}Sn NMR spectroscopy).

Further indication for equilibria that generate ladders, and even monomeric distannoxane units, was obtained using electrospray mass spectrometry (ESMS). Thus, the ESMS spectra (positive mode, cone voltage 200 V) of the double ladder clusters $\{[(Me_3SiCH_2)ClSn(CH_2)_nSnCl(CH_2SiMe_3)]O\}_4$ (M) (**25**–**30**; $n = 5$–8, 10, 12) revealed mass clusters for $[\frac{1}{4}M - Cl]^+$(**a**), $[\frac{1}{2}M - 3Cl + O]^+$ (**b**), $[\frac{1}{2}M - Cl]^+$(**c**), $[M - 2Cl + OH]^+$ (**d**), and $[M - Cl]^+$ (**e**) with the expected isotope patterns. Proposed structures for ions **a**–**e** for **25**–**30** are depicted in Chart 2.

Conclusions

In an effort to answer the question posed in the title, oligomethylene-bridged double ladders $\{[(Me_3SiCH_2)ClSn(CH_2)_nSnCl(CH_2SiMe_3)]O\}_4$ (**25**–**30**; $n = 5$–8, 10, 12) with up to twelve carbon atoms in the spacer were synthesised. It was noted that the yields decreased with increasing spacer lengths from 96% ($n = 5$) to 35% ($n = 12$) in favour of oligomeric or polymeric products, which presumably have random cross-linked structures. In solution the double ladder compounds **26**–**30** are in equilibrium with the ladder compounds $\{[(Me_3SiCH_2)ClSn(CH_2)_nSnCl(CH_2SiMe_3)]O\}_2$ (**31**–**35**; $n = 6$–8, 10, 12), whereby the population of the latter increases along with

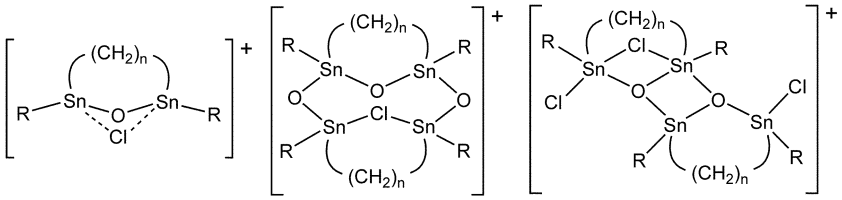

[¼ M - Cl]$^+$ [½ M - 3Cl + O]$^+$ [½ M - Cl]$^+$

25a, n = 5, 533.0	**25b**, n = 5, 1047.0	**25c**, n = 5, 1102.9
26a, n = 6, 547.0	**26b**, n = 6, 1075.0	**26c**, n = 6, 1130.9
27a, n = 7, 561.0	**27b**, n = 7, 1103.0	**27c**, n = 7, 1159.0
28a, n = 8, 575.0	**28b**, n = 8, 1131.1	**28c**, n = 8, 1187.0
29a, n = 10, 603.1	**29b**, n = 10, 1187.1	**29c**, n = 10, 1243.2
30a, n = 12, 631.1	**30b**, n = 12, 1243.2	**30c**, n = 12, 1299.1

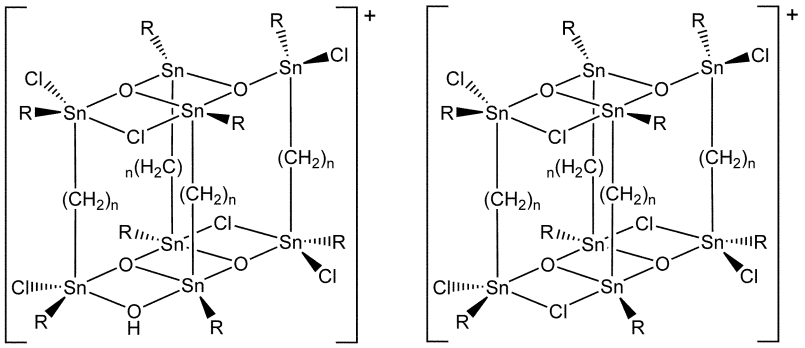

[M - 2Cl + OH]$^+$ [M - Cl]$^+$

25d, n = 5, 2220.8	**25e**, n = 5, 2239.8
26d, n = 6, 2276.9	**26e**, n = 6, 2295.9
27d, n = 7, 2333.0	**27e**, n = 7, 2351.9
28d, n = 8, 2389.0	**28e**, n = 8, 2408.0
29d, n = 10, 2501.1	**29e**, n = 10, 2520.1
30d, n = 12, 2614.3	**30e**, n = 12, 2633.2

R = CH_2SiMe_3

Chart 2

the spacer length *n*. In the context of this equilibrium, it may be interesting for a future investigation to compare the catalytic activity of **25**–**30** in organic reactions, such as transesterifications or the formation of urethane, to get further insights into the operative mechanisms for tetraorganodistannoxane catalysts.[3]

Experimental

General information

Solvents were dried and freshly distilled prior to use. Air-sensitive compounds were handled under vacuum or argon using standard vacuum line and Schlenk techniques. The α,ω-bis(triphenylstannyl)alkanes, $(Ph_3Sn)_2(CH_2)_n$ ($n = 5$–8, 10, 12), were synthesised according to literature procedures.[12] The ^{1}H, ^{13}C, and ^{119}Sn NMR spectra were recorded using Jeol GX 270, Varian 300 Unity Plus and Jeol Eclipse Plus 400 spectrometers and were referenced to $SiMe_4$ (^{1}H, ^{13}C) and $SnMe_4$ (^{119}Sn). The elemental analyses were performed on an instrument from Carlo Erba Strumentazione (Model 1106). The IR spectra were recorded using a BioRad FTIR spectrometer. Electrospray mass spectra were obtained with a Platform II single quadrupole mass spectrometer (Micromass, Altrincham, UK) using an acetonitrile mobile phase. Acetonitrile solutions (0.1 mM) of the compounds were injected directly into the spectrometer *via* a Rheodyne injector equipped with a 50 μL loop. A Harvard 22 syringe pump delivered the solutions to the vaporisation nozzle of the electrospray ion source at a flow rate of 10 μL min^{-1}. Nitrogen was used as both a drying gas and for nebulisation with flow rates of approximately 200 and 20 mL min^{-1}, respectively. Pressure in the mass analyser region was usually about 4×10^{-5} mbar. Typically 10 signal-averaged spectra were collected.

Syntheses

α,ω-Bis(iododiphenylstannyl)alkanes $IPh_2Sn(CH_2)_nSnPh_2I$ (1–6; $n = 5$–8, 10, 12). A solution of iodine (50.8 g, 200.0 mmol) in $CHCl_3$ (2 L) was added dropwise to a magnetically stirred solution of the appropriate $Ph_3Sn(CH_2)_nSnPh_3$ (100.0 mmol) in 200 mL of $CHCl_3$ at 0 °C. After complete addition the solution was allowed to warm to room temperature and was stirred overnight. Removal of the solvent *in vacuo* and the phenyl iodide at 80 °C/10^{-3} Torr for 2 h gave a light brown oil in quantitative yields that was used without purification.

α,ω-Bis[(trimethylsilylmethyl)diphenylstannyl]alkanes $(Me_3SiCH_2)Ph_2Sn(CH_2)_nSnPh_2(CH_2SiMe_3)$ (7–12; $n = 5$–8, 10, 12). A Grignard solution prepared from Me_3SiCH_2Cl (26.99 g, 220.0 mmol) and Mg (5.88 g, 242.0 mmol) in 200 mL THF was added *via* cannula to a solution of the appropriate $IPh_2Sn(CH_2)_nSnPh_2I$ (100.0 mmol) in 400 mL of THF. The

Table 3 Crystal data for **25**, **27**, **29** and **30**

	25	**27**	**29**	**30**
Formula	$C_{52}H_{128}Cl_8O_4Si_8Sn_8$	$C_{60}H_{144}Cl_8O_4Si_8Sn_8$	$C_{72}H_{168}Cl_8O_4Si_8Sn_8 \cdot 5\ C_7H_8$	$C_{80}H_{184}Cl_8O_4Si_8Sn_8 \cdot 2\ C_7H_8$
M	2275.38	2387.59	2878.37	2852.60
Crystal system	Monoclinic	Monoclinic	Monoclinic	Triclinic
Space group	$P2_1/c$	$C2/c$	$C2/c$	$P-1$
a/Å	18.351(2)	38.6254(7)	49.801(1)	13.169(2)
b/Å	24.823(2)	12.3153(2)	25.1497(7)	22.458(6)
c/Å	12.2041(9)	21.5662(5)	12.1328(3)	11.489(1)
α/°	90	90	90	94.79(1)
β/°	94.768(5)	101.3916(7)	100.687(2)	98.670(9)
γ/°	90	90	90	76.67(2)
U/Å^3	5540.0(8)	10 056.6(3)	14 932.5(7)	3264(1)
Z	2	4	4	1
μ/mm^{-1}	2.079	2.295	1.561	1.780
No. reflns collected	26 734	41 657	70 387	15 561
No. indep. reflns	9720	9194	17 007	14 913
No. obsd reflns [$I > 2\sigma(I)$]	2828	4994	5254	9223
R_1 (F) [$I > n\sigma(I)$]	0.074 ($n = 2$)	0.046 ($n = 2$)	0.045 ($n = 3$)	0.053 ($n = 3$)
wR_2 (F^2) (all data)	0.215	0.063	–	–
a	0.0911	0	–	–
wR [$I > 3\sigma(I)$]	–	–	0.048	0.051
g	–	–	0	0.00001

reaction mixture was heated at reflux overnight. After cooling to room temperature and hydrolysing, initially with saturated NH_4Cl solution (50 mL) and then water (200 mL), most of the THF was removed *in vacuo*. The reaction mixture was extracted with diethyl ether (2×400 mL) and the combined organic phases dried over Na_2SO_4. The solution was filtered and the solvent removed *in vacuo*. After heating at 80 °C and 10^{-3} Torr for 2 h to remove all volatiles, a light brown oil was obtained in quantitative yields that was used without purification.

α,ω-Bis[(trimethylsilylmethyl)dichlorostannyl]alkanes (Me_3SiCH_2)$Cl_2Sn(CH_2)_nSnCl_2(CH_2SiMe_3$) (13–18; $n = 5$–8, 10, 12). A suspension of the appropriate $(Me_3SiCH_2)Ph_2Sn(CH_2)_nSnPh_2(CH_2SiMe_3)$ (100.0 mmol) in 500 mL concentrated HCl was stirred overnight at 60 °C. The crude product was extracted with 400 mL of dichloromethane, washed with 1 M HCl (2×100 mL) and dried over Na_2SO_4. After filtering, the solvent was removed *in vacuo* and the residue recrystallised from hexane at −20 °C to give a colourless solid.

α,ω-Bis[(trimethylsilylmethyl)stannoxy]alkanes $Me_3SiCH_2(O)Sn(CH_2)_nSn(O)CH_2SiMe_3$ (19–24; $n = 5$–8, 10, 12). A solution of the appropriate $(Me_3SiCH_2)Cl_2Sn(CH_2)_nSnCl_2(CH_2SiMe_3)$ (30.0 mmol) in 200 mL toluene was combined with a solution of KOH (13.5 g, 240 mmol) in 200 mL H_2O and stirred at reflux overnight. After cooling, the precipitate was collected by filtration, washed with water (1 L) and dried at 80 °C to give a colourless solid.

Oligomethylene-bridged double ladders {[(Me_3SiCH_2)$ClSn(CH_2)_nSnCl(CH_2SiMe_3$)]O}$_4$ (25–30; $n = 5$–8, 10, 12). Equimolar amounts of the appropriate $(Me_3SiCH_2)Cl_2Sn(CH_2)_nSnCl_2(CH_2SiMe_3)$ (1.00 mmol) and $(Me_3SiCH_2)(O)Sn(CH_2)_nSn(O)(CH_2SiMe_3)$ (1.00 mmol) were combined, toluene (100 mL for $n = 5$–7, 500 mL for $n = 8$, 10, 12) added and the reaction mixture stirred for 2 h at room temperature. The solution was then heated to reflux gradually over 6 h and maintained at reflux overnight. Most of the solvent was removed and the solution allowed to cool slowly to give colourless crystals.

Crystallography

Single crystals of **25**, **27**, **29** and **30** suitable for X-ray analysis were obtained from toluene solutions at 4 °C. Crystallographic parameters and refinement details are given in Table 3.§ Intensity data for colourless crystals of **25**, **27**, **29** · 5(toluene) and **30** · 2(toluene) were measured at 173 K on a Nonius Kappa CCD for **25**, **27** and **29** and a Rigaku AFC7R for **30** (measured at the University of Adelaide), using Mo Kα radiation. The structures were solved by heavy-atom methods[13] and refined (anistropic displacement parameters and H atoms in their calculated positions) with a weighting scheme $w = 1/[\sigma^2(F_o^2) + aP^2]$ where $P = (F_o^2 + 2F_c^2)/3$) on F^2 with SHELXL-97 for **25** and **27**,[14] and a weighting scheme of the form $w = 1/[\sigma^2(F_o) + g|F|^2]$ for **29** · 5(toluene) and **30** · 2(toluene) on F using teXsan.[15] Disordered solvent toluene molecules were located in the structures of **29** · 5(toluene) and **30** · 2(toluene) and were modelled as idealised groups.[15] The molecular structures (ORTEP,[16] 35% displacement parameters) are shown in Figs. 1, 3–5. Data manipulation was performed using teXsan.[15]

Acknowledgements

The Australian Research Council, the Deutsche Forschungsgemeinschaft, and the National University of Singapore (R-143-000-186-112) are thanked for their support of this work.

References

1 (*a*) A. G. Davies, *Organotin Chemistry*, VCH, Weinheim, 1997; (*b*) D. Dakternieks, K. Jurkschat, S. van Dreumel and E. R. T. Tiekink, *Inorg. Chem.*, 1997, **36**, 2023; (*c*) J. Beckmann, M. Biesemans, K. Hassler, K. Jurkschat, J. C. Martins, M. Schürmann and R. Willem, *Inorg. Chem.*, 1998, **37**, 4891; (*d*) J. Beckmann, K. Jurkschat, U. Kaltenbrunner, S. Rabe, M. Schürmann, D. Dakternieks, A. Duthie and D. Müller, *Organometallics*, 2000, **19**, 4887; (*e*) K. Sakamoto, H. Ikeda, H. Akashi, T. Fukuyama, A. Orita and J. Otera, *Organometallics*, 2000, **19**, 3242; (*f*) A. Orita, J. Xiang, K. Sakamoto and J. Otera, *J. Organomet. Chem.*, 2001, **624**, 287; (*g*) J. Beckmann, K. Jurkschat, S. Rabe, M. Schürmann and D. Dakternieks, *Z. Anorg. Allg. Chem.*, 2001, **627**, 458; (*h*) J. Beckmann, M. Henn, K. Jurkschat, M. Schürmann, D. Dakternieks and A. Duthie, *Organometallics*,

§ CCDC reference numbers 240117–240120. See http://www.rsc.org/suppdata/nj/b3/b316009b/ for crystallographic data in .cif or other electronic format.

2002, **21**, 192; (*i*) U. Baumeister, D. Dakternieks, K. Jurkschat and M. Schürmann, *Main Group Met. Chem.*, 2002, **25**, 521; (*j*) J. Beckmann, D. Dakternieks, F. S. Kuan and E. R. T. Tiekink, *J. Organomet. Chem.*, 2002, **659**, 73; (*k*) J. Beckmann, D. Dakternieks, A. Duthie, K. Jurkschat and M. Schürmann, *Z. Anorg. Allg. Chem.*, 2003, **629**, 99; (*l*) J. Beckmann, D. Dakternieks, A. Duthie and E. R. T. Tiekink, *J. Chem. Soc., Dalton Trans.*, 2003, 755; (*m*) J. Beckmann, D. Dakternieks, A. Duthie and C. Mitchell, *Appl. Organomet. Chem.*, 2004, **18**, 51.

2 (*a*) H. Nozaki and J. Otera, in *Organometallics in Organic Synthesis*, eds. A. de Meijere and H. tom Dieck, Springer, Berlin, 1987, p. 169; (*b*) J. Otera, in *Advances in Detailed Reaction Mechanims*, ed. J. M. Coxon, JAI Press, Inc., Greenwhich, 1994, vol. **3**, p. 167; (*c*) T. Kobayashi, A. Yamaguchi, T. Hagiwara and Y. Hori, *Polymer*, 1995, **36**, 4707; (*d*) Y. Hori, Y. Gonda, Y. Takahashi and T. Hagiwara, *Macromolecules*, 1996, **29**, 804; (*e*) A. Orita, A. Mitsutome and J. Otera, *J. Org. Chem.*, 1998, **63**, 2420; (*f*) Y. Hori and T. Hagiwara, *Int. J. Biol. Macromol.*, 1999, **25**, 237; (*g*) X. Q. Liu, Z. C. Li, F. S. Du and F. M. Li, *Polym. Bull.*, 1999, **42**, 649; (*h*) A. Orita, T. Ito, Y. Yasui and J. Otera, *Synlett*, 1999, **12**, 1927; (*i*) S. Hiki, M. Miyamoto and Y. Kimura, *Polymer*, 2000, **41**, 7369; (*j*) H. Takahashi, T. Hayakawa and M. Ueda, *Chem. Lett.*, 2000, 684; (*k*) R. Nagahata, J. I. Sugiyama, M. Goyal, M. Asai, M. Ueda and K. Takeuchi, *J. Polym. Sci., Part A: Polym. Chem.*, 2000, **38**, 3360; (*l*) A. Nishio, A. Mochizuki, J. I. Sugiyama, K. Takeuchi, M. Asai, K. Yonetake and M. Ueda, *J. Polym. Sci., Part A: Polym. Chem.*, 2001, **39**, 416; (*m*) S. Durand, K. Sakamoto, T. Fukuyama, A. Orita, J. Otera, A. Duthie, D. Dakternieks, M. Schulte and K. Jurkschat, *Organometallics*, 2000, **19**, 3220; (*n*) M. Ishii, M. Okazaki, Y. Shibasaki, H. Takahashi, T. Hayakawa and M. Ueda, *Polym. Prepr.*, 2001, **42**, 462; (*o*) B. Jousseaume, C. Laporte, M. C. Rascle and T. Toupance, *Chem. Commun.*, 2003, 1425.

3 (*a*) R. P. Houghton and A. W. Mulvaney, *J. Organomet. Chem.*, 1996, **517**, 107; (*b*) R. P. Houghton and A. W. Mulvaney, *J. Organomet. Chem.*, 1996, **518**, 21.

4 (*a*) D. Dakternieks, K. Jurkschat, D. Schollmeyer and H. Wu, *Organometallics*, 1994, **13**, 4121; (*b*) M. Mehring, M. Schürmann, H. Reuter, D. Dakternieks and K. Jurkschat, *Angew. Chem., Int. Ed.*, 1997, **36**, 1112; (*c*) M. Mehring, M. Schürmann, I. Paulus, D. Horn, K. Jurkschat, A. Orita, J. Otera, D. Dakternieks and A. Duthie, *J. Organomet. Chem.*, 1999, **574**, 176; (*d*) M. Schulte, M. Schürmann, D. Dakternieks and K. Jurkschat, *Chem. Commun.*, 1999, 1291; (*e*) M. Mehring, I. Paulus, B. Zobel, M. Schürmann, K. Jurkschat, A. Duthie and D. Dakternieks, *Eur. J. Inorg. Chem.*, 2001, 153; (*f*) B. Costisella, D. Dakternieks, K. Jurkschat, M. Mehring, I. Paulus and M. Schürmann, *Chem. Heterocycl. Compd. (N. Y.)*, 2001, **11**, 1535; (*g*) M. Mehring, G. Guiseppina, S. Hadjikakou, M. Schürmann, D. Dakternieks and K. Jurkschat, *Chem. Commun.*, 2002, 834; (*h*) J. Beckmann, D. Dakternieks, A. Duthie, F. S. Kuan and E. R. T. Tiekink, *Organometallics*, 2003, **22**, 4399.

5 J. Beckmann, D. Dakternieks, A. Duthie, F. S. Kuan and E. R. T. Tiekink, *J. Organomet. Chem.*, 2003, **688**, 56.

6 A. Szabó, D. Gournis, M. A. Karakassides and D. Petridis, *Chem. Mater.*, 1998, **10**, 639.

7 (*a*) R. K. Ingham, S. D. Rosenberg and H. Gilman, *Chem. Rev.*, 1960, **60**, 459; (*b*) L. H. Lohmann, *J. Organomet. Chem.*, 1965, **4**, 382; (*c*) R. K. Harris and A. Sebald, *J. Organomet. Chem.*, 1987, **331**, C9.

8 M. C. Janzen, M. C. Jennings and R. J. Puddephatt, *Organometallics*, 2001, **20**, 4100.

9 (*a*) P. G. Harrison, M. J. Begley and K. C. Molloy, *J. Organomet. Chem.*, 1980, **186**, 213; (*b*) D. Dakternieks, R. W. Gable and B. F. Hoskins, *Inorg. Chim. Acta*, 1985, **85**, L43.

10 (*a*) J. Otera, T. Yano, K. Nakashima and R. Okawara, *Chem. Lett.*, 1984, 2109; (*b*) T. Yano, K. Nakashima, J. Otera and R. Okawara, *Organometallics*, 1985, **4**, 1501; (*c*) V. K. Jain, V. B. Mokal and P. Sandor, *Magn. Reson. Chem.*, 1992, **30**, 1158; (*d*) D. C. Gross, *Inorg. Chem.*, 1989, **28**, 2355; (*e*) D. L. Tierney, P. J. Moehs and D. L. Hasha, *J. Organomet. Chem.*, 2001, **620**, 211; (*f*) D. L. Hasha, *J. Organomet. Chem.*, 2001, **620**, 296.

11 B. Zobel, M. Schürmann, K. Jurkschat, D. Dakternieks and A. Duthie, *Organometallics*, 1998, **17**, 4096.

12 (*a*) H. Zimmer and J. J. Miller, *Naturwissenschaften*, 1966, **53**, 38; (*b*) Y. Azuma and M. Newcomb, *Organometallics*, 1984, **3**, 9; (*c*) M. T. Blanda, J. H. Horner and M. Newcomb, *J. Org. Chem.*, 1989, **54**, 4626.

13 (*a*) G. M. Sheldrick, *Acta Crystallogr., Sect. A*, 1990, **46**, 467; (*b*) P. T. Beurskens, G. Admiraal, G. Beurskens, W. P. Bosman, S. García-Granda, J. M. M. Smits and C. Smykalla, *The DIRDIF program system*, Technical Report of the Crystallography Laboratory, University of Nijmegen, The Netherlands, 1992.

14 G. M. Sheldrick, *SHELXL-97, Program for refinement of crystal structures*, University of Göttingen, Germany, 1997.

15 *teXsan: Single Crystal Structure Analysis Software*, Version 1.7, Molecular Structure Corporation, The Woodlands, TX, USA, 1997.

16 C. K. Johnson, *ORTEP-II: A FORTRAN Thermal Ellipsoid Plot Program for Crystal Structure Illustrations*, Report ORNL-5138, Oak Ridge National Laboratory, Oak Ridge, TN, USA, 1976.